


Role of nano-magnetized *Citrus X sinensis* (orange) peels for decontamination of pendimethalin from aqueous resources: a comparative study of untreated and carbonaceous orange peels with nano-magnetized peels

Shafaq Mubarak ^{a,*}, Bilal Ashraf^b and Amina Asghar^b

^a Applied Chemistry Research Center, PCSIR, Lahore, Pakistan

^b Division of Science and Technology, Department of Chemistry, University of Education, Township, Lahore, Pakistan

*Corresponding author. E-mail: shafaq.mubarak@gmail.com

 SM, 0000-0003-4122-9277

ABSTRACT

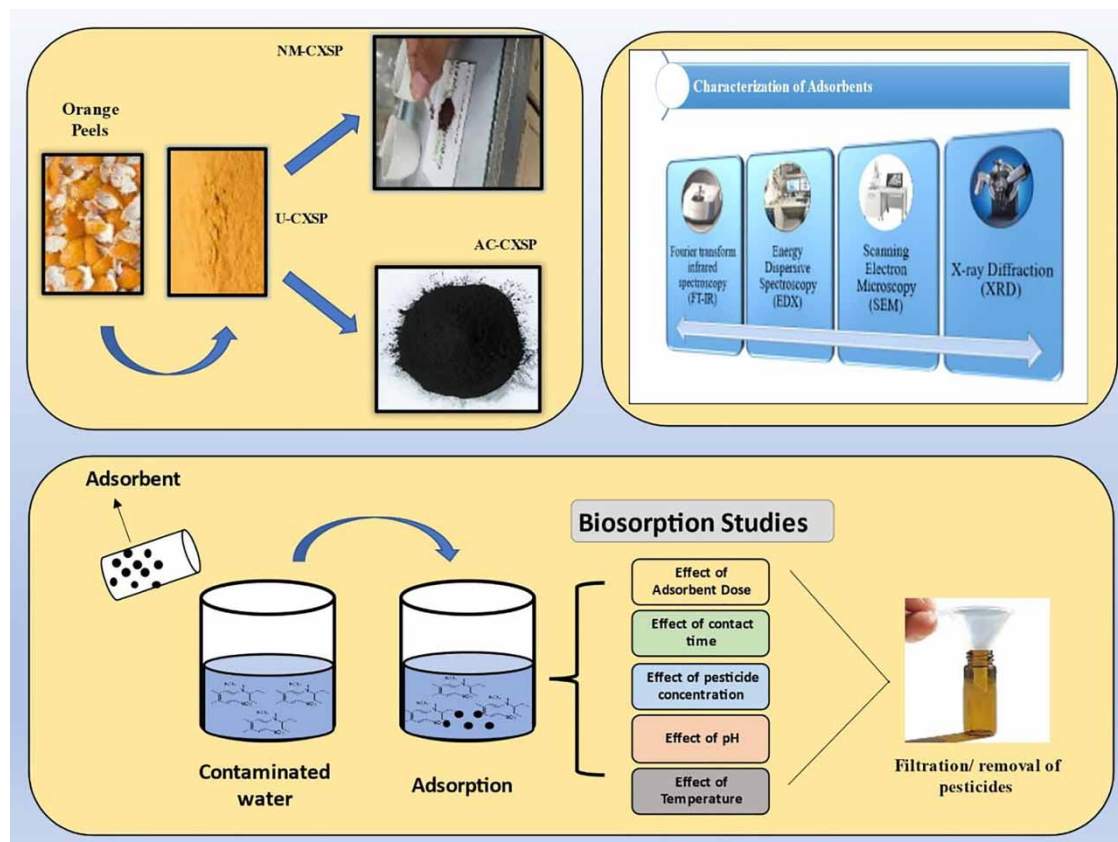
Biosorption is a low-cost, environment friendly wastewater treatment method that involves a simple procedure for the removal of pesticides and their residues from wastewater. In the present investigation, untreated *Citrus X sinensis* peels (U-CXSP), activated carbon *Citrus X sinensis* peels (AC-CXSP) and nano-magnetized *Citrus X sinensis* peels (NM-CXSP) adsorbents were applied for the uptake of pendimethalin (PDM) from aqueous resources. The laboratory-prepared adsorbents were characterized using SEM, EDX, FTIR, VSM and XRD. Biosorption studies were carried out by varying different parameters, i.e., adsorbents dosage (0.1–0.5 g), time of contact (10–70 min), initial concentration of PDM (5–200 ppm), pH and temperature. The results showed that the removal efficiency of U-CXSP was increased from 97 to 114 mg/g for AC-CXSP adsorbent and increased from 97 to 111 mg/g for NM-CXSP adsorbent. Kinetics data obtained from this study well fitted with pseudo-second-order kinetic model. Adsorption isotherms were studied and the adsorption data well fitted with Langmuir and Freundlich models. Order of the adsorption efficiency is observed as follows: AC-CXSP > NM-CXSP > U-CXSP.

Key words: adsorption, *Citrus X sinensis* (orange) peels, magnetization, wastewater treatment

HIGHLIGHTS

- Biosorption is a cost-effective technique that can eliminate pesticides and their remnants from wastewater.
- For the first time, nano-magnetic *Citrus X sinensis* peels are employed to mitigate pendimethalin from aqueous resources in this study.
- Magnetized nano-adsorbent proved to be more efficient as compared to untreated orange peels for the uptake of pesticides.

GRAPHICAL ABSTRACT



1. INTRODUCTION

In the present era, pesticide contamination of groundwater, surface water and soils is a major problem across the world as many of these compounds are hazardous for both human and environmental health. Pesticide usage in agriculture and home pest control operations is increasing and thus damaging the water resources day-by-day (Memon *et al.* 2008). Wind erosion, industrial discharges, surface runoff, leaching and variety of other sources all contribute to this pollution. As a result, pesticides are found in water bodies in many countries throughout the world. Residual pesticides are particularly a strong family of water contaminants since they are often non-biodegradable. Pesticides are also carcinogenic by nature. As a result of their toxicity, pesticides and their breakdown products pose a potential threat by polluting the environment. Pesticides are employed in agricultural crops globally in an estimated 2.5 million tonnes per year resulting in higher amount of residual pesticides in runoff water. In most studies, fewer than 0.3% of the administered pesticides reach the target insect, implying that 99.7% of them end up elsewhere in the environment (Bulgariu *et al.* 2019).

Pendimethalin is a chlorinated herbicide that is used in more than 80 countries and is arguably the most widely used herbicide in the world. Pendimethalin is a dinitroaniline herbicide, which works as a microtubule disruptor in plants, which stops elongation and cell division. It is practically non-volatile, with a half-life of 30–90 days in soil; however, this varies depending on environmental conditions such as moisture content, pH, microbial activity and temperature. It is used before emergence on maize, rice and cereals, as well as before sowing cotton, bean, groundnuts and soya bean with shallow soil absorption. Pendimethalin is transmitted to surface and subsurface water bodies due to its high persistence and mobility, and has been identified in ground water, drinking water, high alpine lakes, rain water and rivers (Ayuba & Nyijime 2021a, 2021b).

A number of techniques have been employed for the treatment of water contaminated with pendimethalin. These include sedimentation, coagulation, microfiltration, ultra-centrifugation and flocculation (Jabłońska 2012). However, these procedures are linked to a high level of risk, operation expenses and sludge production which need further treatment.

Adsorption involving fruit peels as adsorbents is an effective technique for treating inorganic- and organic-pollutant-contaminated water (Moradi *et al.* 2014). Agricultural-based materials as adsorbents are a possible option for wastewater treatment because they have various benefits, which include abundant availability, low manufacturing costs, capacity to reuse, high removal efficiency and easy preparation stages (Kushwaha *et al.* 2013). More efficient and readily accessible biomaterials, such as orange peels, are available as waste from companies and juice stores in enormous quantities (Biswas *et al.* 2008). Adsorption of metals and hazardous materials has done by using activated carbon produced from orange peels as an adsorbent (Ren *et al.* 2011; Salman *et al.* 2011). As well as, the chemical treatment of orange peels caused an increase in their efficiency for the uptake of contaminants from water. For the first time, nano-magnetic *Citrus X sinensis* peels (NM-CXSP) are employed to mitigate pendimethalin from aqueous resources in this study. Batch sorption/isotherms investigations are used to compare this nano-magnetized bio-sorbent to untreated *Citrus X sinensis* peels (U-CXSP). To study the kinetics of the adsorption phenomena, pseudo-first-order, pseudo-second-order and intraparticle diffusion models were used. This work is a follow-up to our previously published work (Asghar *et al.* 2024), in which we removed chlorpyrifos using orange peels.

2. METHODOLOGY

2.1. Reagents/chemicals

All reagents/chemicals (NH_3 , NaOH , HCl , FeCl_2 , FeCl_3 , NH_3) of analytical grade and adsorbate (pendimethalin) were procured from Sigma Aldrich and Merck.

2.2. Preparation of bio-sorbents

2.2.1. Preparation of U-CXSP

Citrus X sinensis peels (biowaste) were collected from several marketplaces in city Lahore, Pakistan. The peels were cleaned and chopped into tiny pieces and washed with tap water. Peels were sun-dried for 2 days before being further dried at $120\text{ }^\circ\text{C}$ for 1–2 days in oven. Dried peels were ground into powder form and sieved using a 100 BSS (British Standard Sieves) sieve. The prepared U-CXSP is employed for further analysis/treatment.

2.2.2. Preparation of AC-CXSP

To make activated carbon *Citrus X sinensis* peels (AC-CXSP) from raw *Citrus X sinensis* peels, the dried pieces were placed in a traditional mud pot. Two holes were drilled in the lid, one of which was filled with a tube attached to a nitrogen cylinder and clayed in place. The lid placed on top of the jar to make it airtight and sealed in place with clay. Nitrogen flow was switched on, and nitrogen was allowed to flow for 3 min through the vessel. During the carbonization process, once the nitrogen flow was turned off, the second hole was quickly filled with mud preventing the vessel from entering air.

2.2.3. Preparation of NM-CXSP

The co-precipitation technique was used to make the NM-CXSP adsorbent. Orange peels (30 g) were placed in a flask containing 500 mL of water. $\text{FeCl}_2 \cdot 2\text{H}_2\text{O}$ (36 g) and $\text{FeCl}_3 \cdot 6\text{H}_2\text{O}$ (30 g) solutions (prepared in 500 mL separately) were added drop by drop via a separating funnel. At $60\text{ }^\circ\text{C}$, the solution is agitated continuously for 3–4 h. The pH of the solution was increased to 10 after complete addition by adding ammonia solution (10%) drop by drop. The solution was filtered, and the precipitates were washed in water until they became neutral. Precipitates were dried at $90\text{ }^\circ\text{C}$ before being heated in furnace at $550\text{ }^\circ\text{C}$.

2.3. Characterization of adsorbents prepared

The range of the FTIR spectrometer (Spectrum-2) with ATR assembly of Perkin Elmer FTIR was tuned between $4,000$ and 350 cm^{-1} in a transmission mode using 10 kPa of compressed KBr pellets for functional groups analysis. Magnetic properties were measured at $25\text{ }^\circ\text{C}$ in a magnetic field of 15,000 Oe using a quantum design VSM magnetometer. A Quanta 200 FEG scanning electron microscope (SEM) was used to examine the morphology of adsorbents. The EDX method was used to examine S50 FEI for elemental configuration of adsorbents. The structural study of adsorbents was performed using a PANAlytical eXpert Pro DY3805 Powder XRD.

2.4. Stock solution of pendimethalin

Pendimethalin (0.1 g) was dissolved in 1 L of acetone:water (30:70) combination to make a stock solution (1,000 ppm). With the help of dilution formula, this stock solution was used for further experiments.

2.5. Adsorption studies

Adsorption phenomena were investigated altering a variety of variables, i.e., temperature, adsorbent dose, contact time, pH and starting PDM concentration. The reaction mixtures were filtered and checked for the percentage removal of pendimethalin. The adsorption capacity of each prepared adsorbent for PDM was calculated, as

$$q_e = \frac{(C_i - C_e) * V}{m} \quad (1)$$

Here, ' q_e ' indicates the adsorption capability of adsorbent, ' C_i ' indicates the starting concentration of PDM solution, ' C_e ' indicates the concentration of PDM at equilibrium. ' V ' indicates the solution volume and ' m ' represents the amount of adsorbent used.

The impact of the adsorbent dose was investigated by altering the dose between 0.1 and 0.5 g, and added to a 25-mL solution in 100-mL conical flasks of 0.1 ppm solution of PDM at constant temperature and pH. The effect of contact time was studied by taking 0.1 g of adsorbent in 100-mL flask containing 25-mL solution of 1 ppm pendimethalin. The contact time was varied between 10 and 70 min at a constant temperature and pH. The kinetic data of the study were used to determine the reaction kinetics based on pseudo-first-order, pseudo-second-order and intraparticle diffusion. Effect of initial concentration on adsorption was studied by taking solutions of different concentrations of PDM solution in different flasks for 30 min at constant temperature and pH. Adsorption isotherms (Langmuir and Freundlich) were carried out to investigate the efficiency of each adsorbent separately. The pH of PDM solution was varied between (2 and 10) to check its effect on adsorption using 0.1-M NaOH and HCl solutions. The mixtures were stirred continuously for 30 min at constant temperature. Temperature effects on adsorption were investigated by varying the temperature from 25 to 50 °C.

3. RESULTS AND DISCUSSION

3.1. Characterization

3.1.1. FTIR analysis

The FTIR spectra for prepared adsorbents U-CXSP, AC-CXSP and NM-CXSP are shown in Figure 1. FTIR spectra of U-CXSP represent a signal at 3,338 cm^{-1} that is ascribed to O–H stretching (Mohammad *et al.* 2015; Kadam *et al.* 2020). Alcohols, phenols, acids, ethers and esters absorb at 1,047 cm^{-1} , indicating C–O stretching vibrations (Nandiyanto *et al.* 2019; Abdelhameed *et al.* 2020; Siddique *et al.* 2020). AC-CXSP's FTIR spectra showed some of the same absorption peaks for U-CXSP but the number of peaks in AC-CXSP are absent when compared to U-CXSP, for example, the peak at 3,338 cm^{-1} is missing, indicating a lack of hydroxyl groups in AC-CXSP, and there is also a missing minor peak at 1,602 cm^{-1} , indicating carboxylic group disintegration (Fernandez *et al.* 2014). A peak at 540 cm^{-1} is observed in the FTIR spectra of NM-CXSP, which is attributed to the existence of Fe–O bonds (Shehzad *et al.* 2018). The presence of iron oxide in NM-CXSP is indicated by the emergence of a peak at 540 cm^{-1} . The C–O stretching caused another large vibration in NM-CXSP at 1,087 cm^{-1} . These groups performed a crucial part in pesticide adsorption. The whole FT-IR spectrum revealed that NM-CXSP were successfully synthesized.

3.1.2. SEM-EDX analysis of prepared adsorbents

Morphology of U-CXSP and NM-CXSP is done on SEM at 10.00 kV of accelerated voltage. Both the adsorbents exhibit very diverse porous structures (Shehzad *et al.* 2018), as shown in Figure 2. Considerable changes in the morphology of both adsorbents were detected. The exterior surface of U-CXSP is rather uneven in micrographs, whereas the external surface of NM-CXSP is beautifully patterned, indicating that they are made up of numerous small nanoparticles (Abdelhameed *et al.* 2020). When these tiny primary nanoparticles are combined, they can produce a vast number of pores, resulting in a large microporous volume. The chemical compositions of U-CXSP and NM-CXSP are shown in Figure 3 using Energy Dispersive Spectroscopy (EDX). The results demonstrate that carbon and oxygen have higher values, indicating that organic matter accounts for over 97% of the content of *Citrus X sinensis* peels (Abdelhameed *et al.* 2020). After magnetization, the chemical composition of untreated orange peels revealed a larger proportion of Fe and O, indicating that iron oxide was successfully doped on untreated orange peels (Shehzad *et al.* 2018).

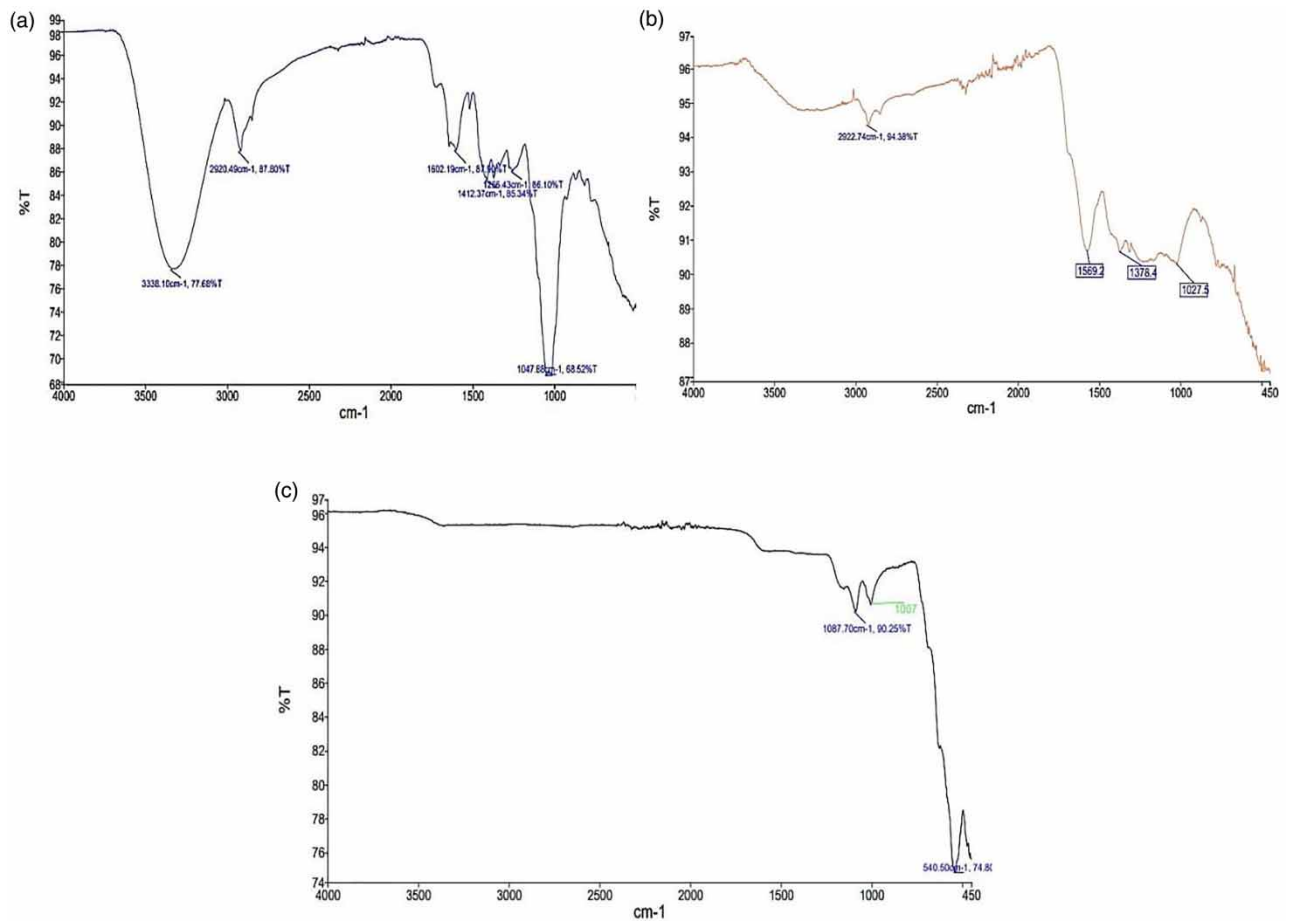


Figure 1 | FTIR analysis of (a) U-CXSP, (b) AC-CXSP and (c) NM-CXSP.

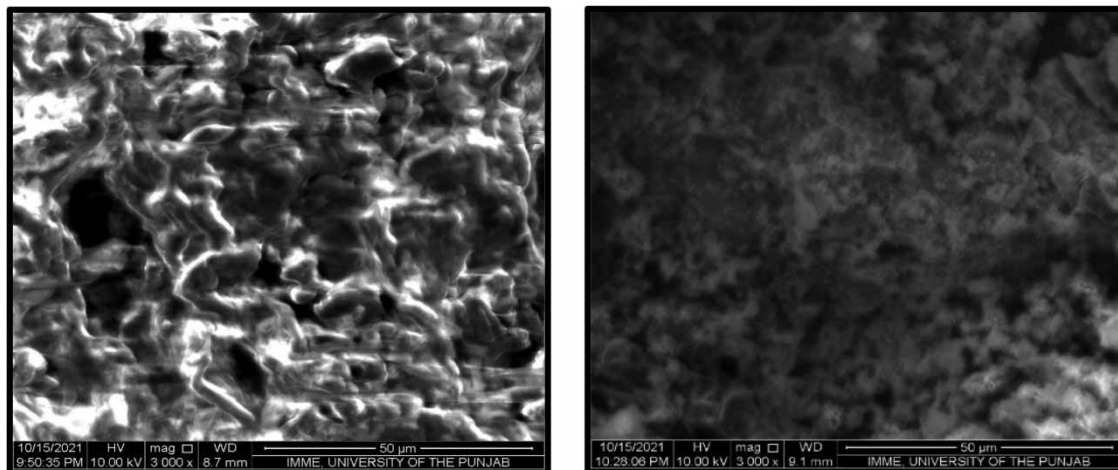


Figure 2 | SEM micrographs of (a) CXSP and (b) NM-CXSP.

3.1.3. XRD analysis

Figure 4 illustrates the XRD (X-ray diffraction) of U-CXSP, AC-CXSP and NM-CXSP, which gave structural information. In XRD, the crystalline material produces a succession of discrete peaks, whereas the amorphous material produces a wide background pattern (Combo *et al.* 2013). The particle size study revealed that the average size of NM-CXSP was in the

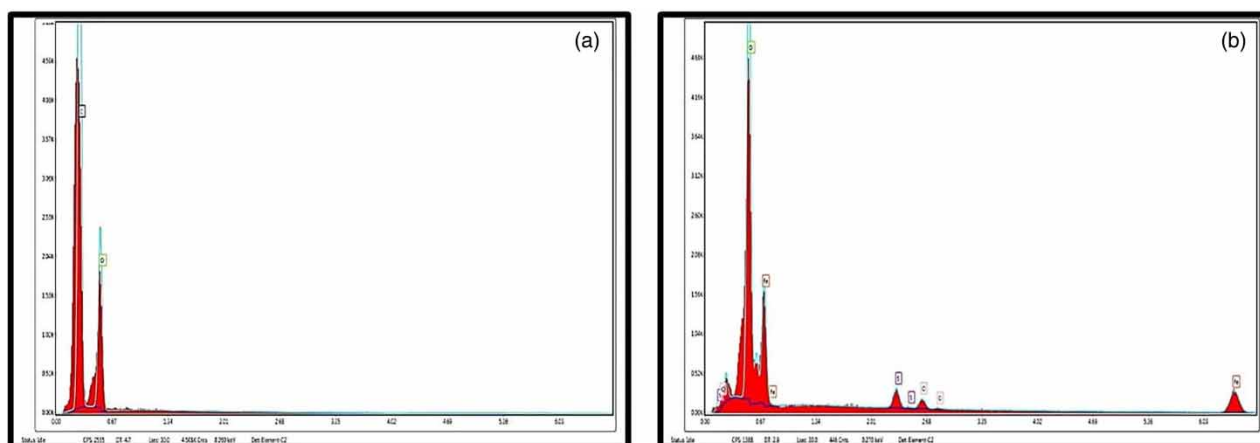


Figure 3 | EDX spectra for (a) U-CXSP and (b) NM-CXSP.

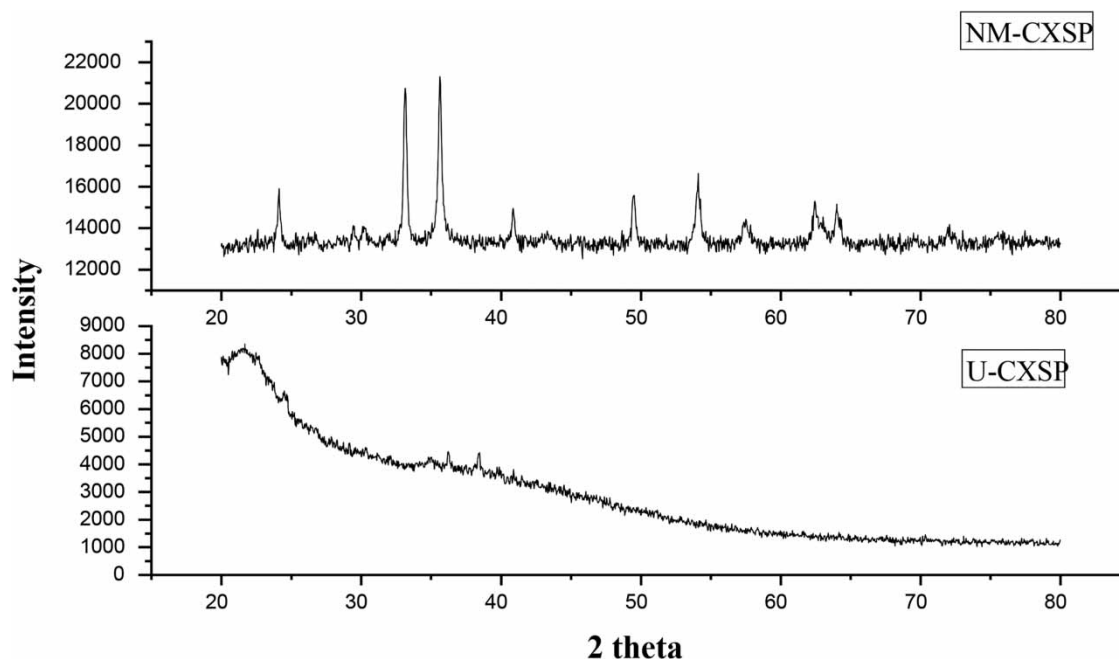


Figure 4 | XRD of U-CXSP and NM-CXSP.

nanometre range, confirming the formation of NM-CXSP. The major phase in the synthesized composite (JCPDS # 89-0688) was magnetite (Fe_3O_4), according to the NM-CXSP diffractogram. At 62.4, 56.8, 43.0, 35.3 and 30.0, Fe_3O_4 has five different peaks that correspond to their indices (4 4 0), (5 1 1), (4 0 0), (3 1 1) and (2 2 0) (Shehzad *et al.* 2018).

3.1.4. VSM analysis

Two magnetic properties of NM-CXSP to examine using a magnetic hysteresis loop (Figure 5) are coercivity (H_c) and saturation magnetization (M_s). The saturation magnetization and coercivity were determined to be 160 Oe and 94 emu g^{-1} , respectively. Coercivity of NM-CXSPs was found to be >100 Oe, with coercivity being regulated by a variety of factors such as magnetic shape size distribution, anisotropy, particle morphology, magnetic domain size, micro-strain and magneto crystalline anisotropy. It is also usual to see a direct link between coercivity and porosity. The more the porosity the greater the coercivity. As a consequence, the adsorption capacity of NM-CXSP has enhanced.

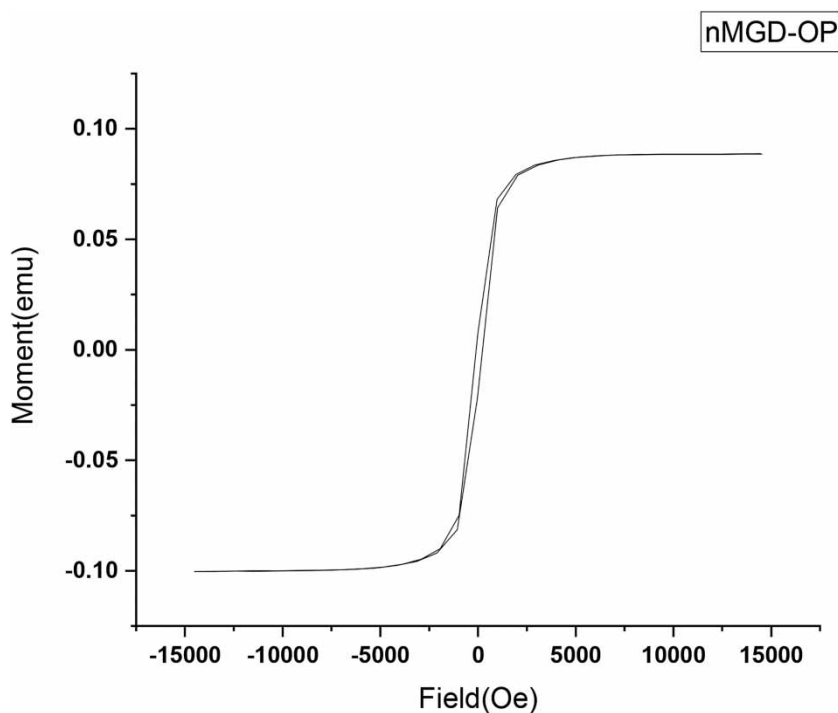


Figure 5 | VSM of NM-CXSP.

3.2 .Factors affecting adsorption of pendimethalin

3.2.1. Adsorbent dosage effect

The adsorbent dosage effect was analyzed by taking the dose in the range of 0.1–0.5 g, and the studies were conducted out at a fixed starting adsorbate concentration (0.1 ppm), temperature 25 °C and pH = 7. Results in Figure 6 show that at the start with the increase in adsorbent dosage the percentage adsorption was increased up to 0.3 g. This increase in percentage adsorption is attributed to the fact that as the dose of adsorbent is increased a larger number of adsorption sites became available. After 0.3 g of adsorbent dosage, there is no significant change observed which is due to the reason that all the adsorbate molecules

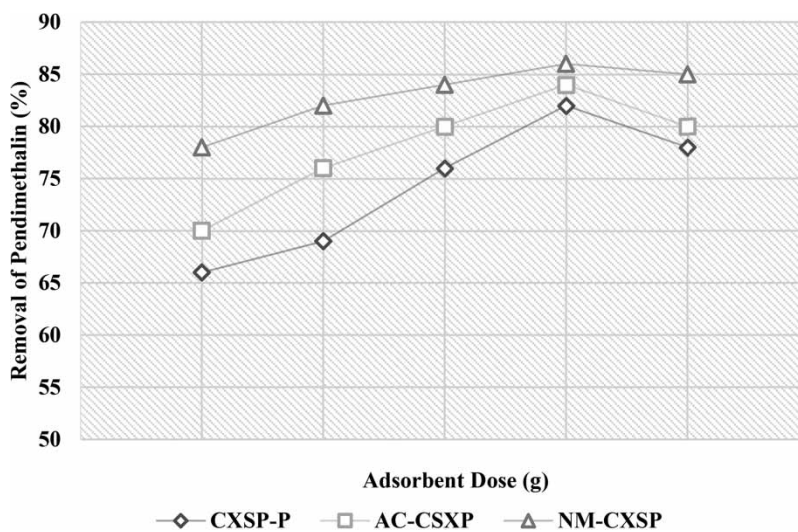


Figure 6 | Effect of adsorbent dose for pendimethalin uptake (pesticide's concentration = 0.1 ppm, contact time = 30 min, temperature = 25 °C, pH = 7).

got adsorbed on available sites of adsorbent. There are no further interactions between adsorbent and the adsorbate (Hameed *et al.* 2009; Abdelhameed *et al.* 2020).

3.2.2. PDM concentration effect

The starting concentration of PDM solution can also affect the adsorption phenomenon, it was investigated by varying the concentration of pendimethalin in between 5 and 200 ppm. All the experiments were done by keeping the adsorbent dosage constant at 0.1 g with continuous stirring for 30 min at constant temperature, i.e., 25 °C. At the start, increase in concentration causes an increase in adsorption percentage of up to 80 ppm solution of pendimethalin. After this concentration, further increase in concentration did not cause a significant increase in percentage adsorption. This is attributed to the fact that all the active sites available for the adsorbate molecules became occupied up to 80 ppm due to which there is no significant change observed in percentage adsorption after 80 ppm of concentration.

Adsorption capacity of the adsorbents prepared (U-CXSP, AC-CXSP and NM-CXSP) for the uptake of PDM was checked by studying the isotherm models (Langmuir and Freundlich). The equations used for the Langmuir and Freundlich isotherm models are given in the following:

$$q_e = \frac{q_m C_e K_L}{(1 + C_e K_L)} \quad (2)$$

$$\frac{C_e}{q_e} = \frac{1}{q_{\max} b} + \frac{C_e K_L}{q_{\max}} \quad (3)$$

where ' q_e ' indicates the adsorption capability at equilibrium, ' q_m ' indicates the pendimethalin maximal adsorption capacity and K_L indicates the equilibrium constant (Enniya *et al.* 2018).

$$q_e = K C_e^{1/n} \quad (4)$$

$$\text{Log} q_e = \text{Log} K + 1/n C_e \quad (5)$$

where ' K ' indicates the Freundlich constant for adsorption capacity bearing unit ($\text{mg}^{1-n} \text{L}^n / \text{g}$) and ' n ' indicates the bond distribution also known as heterogeneity factor (Enniya *et al.* 2018).

The Langmuir isotherm plots for all the adsorbents (U-CXSP, AC-CXSP and NM-CXSP) for the uptake of pendimethalin studied by plotting ' C_e ' along abscissa and ' C_e/q_e ' along ordinate, and the plots are shown in Figure 7. Freundlich isotherm plots were studied by plotting ' $\text{Log} C_e$ ' along x -axis and ' $\text{Log} q_e$ ' along y -axis, and the plots are shown in Figure 8. The parameters like regression factor R^2 and q_{\max} are calculated and are shown in Table 1. According to the findings, both isotherm models best suited the data obtained.

The separation factor describes the major aspect of the Langmuir isotherm ' R_L ' ($R_L = 1/(1 + K_L C_0)$), a dimensionless constant. Irreversible adsorption is observed by $R_L = 0$, favorable adsorption is observed when $0 < R_L < 1$, linear adsorption is denoted by $R_L = 1$ and unfavorable adsorption is denoted by $R_L > 1$ (Sheng *et al.* 2014). In our study, the computed values of R_L were in the range of $0 < R_L < 1$, showing that PDM adsorption on each adsorbent is favorable.

Table 2 shows the comparison of adsorption capacity of U-CXSP, AC-CXSP and NM-CXSP for pendimethalin with other reported low-cost adsorbents.

3.2.3. Effect of reaction time

The impact of contact time on pendimethalin adsorption was studied by varying the contact period from 10 to 70 min. The reactions were carried out with a constant adsorbent dosage and pesticide solution concentration, i.e., 0.1 g and 0.1 ppm respectively. It is found that increasing the contact duration increased the adsorption percentage up to 30 min. The increase in adsorption percentage was ascribed to the fact that as the contact time was increased the adsorbate molecules have a better probability of being adsorbed by the adsorbent surface as time goes on (Kumar and Philip 2006). After 30 min of contact time, the chances of the adsorbate molecules to make contact with the active sites becomes less as all the available active sites of adsorbents became occupied and there are chances of repulsive forces between the adsorbate molecules and the surface of adsorbent (Sheng *et al.* 2014; Enniya *et al.* 2018).

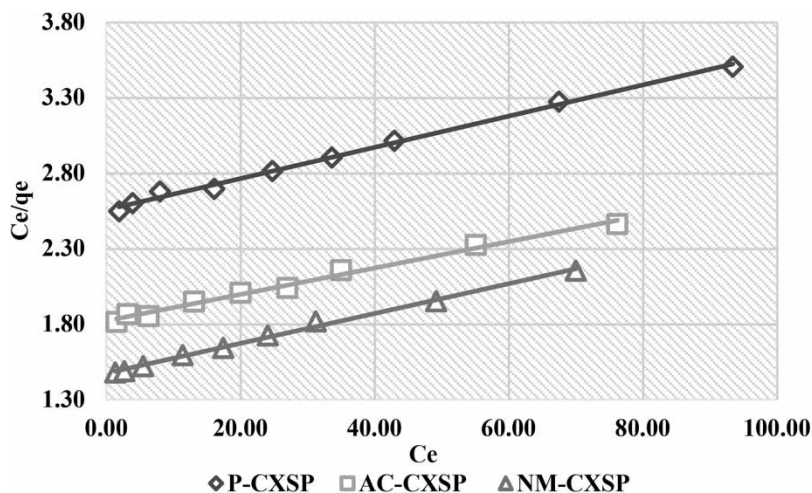


Figure 7 | Langmuir isotherms for adsorption of pendimethalin on U-CXSP, AC-CXSP and NM-CXSP. Experimental conditions: temperature = 25 °C, contact time = 30 min, adsorbent dose = 0.1 g, pH = 7.

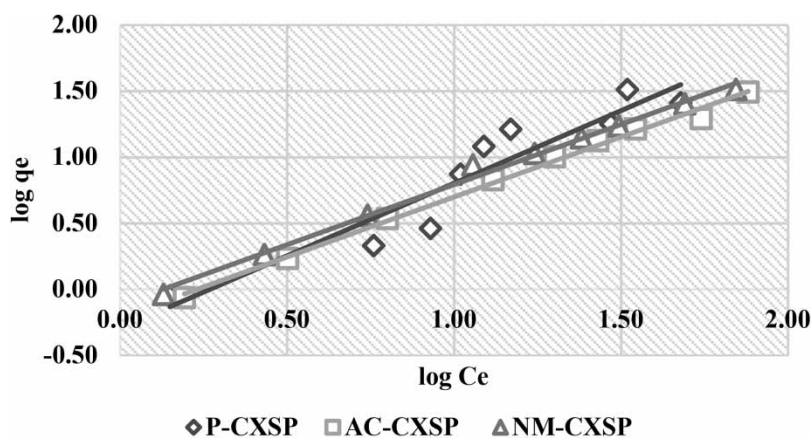


Figure 8 | Freundlich isotherms for adsorption of pendimethalin on U-CXSP, AC-CXSP and NM-CXSP. Experimental conditions: temperature = 25 °C, contact time = 30 min, adsorbent dose = 0.1 g, pH = 7.

Table 1 | Parameters for Langmuir and Freundlich isotherms

| | Langmuir isotherm parameters | | | Freundlich isotherm parameters | | |
|---------|------------------------------|------------|-------|--------------------------------|-------|-------|
| | q_{max} (mg/g) | b (L/mg) | R^2 | K_L | N | R^2 |
| U-CXSP | 97 | 0.004 | 0.994 | 1.6 | 1.081 | 0.998 |
| AC-CXSP | 114 | 0.004 | 0.990 | 1.61 | 1.10 | 0.995 |
| NM-CXSP | 111 | 0.006 | 0.995 | 1.28 | 1.110 | 0.994 |

The kinetic experiments of pendimethalin adsorption on each of the produced adsorbents were carried out individually. Equations (6)–(8) depict for pseudo-first-order, pseudo-second-order and intraparticle diffusion, respectively:

$$\log(q_e - q_t) = \frac{\log q_e - k_1 t}{2.303} \quad (6)$$

Table 2 | Comparison of adsorption capacity of U-CXSP, AC-CXSP and NM-CXSP for pendimethalin with other reported low-cost adsorbents

| Adsorbents | q_{\max} (mg/g) | Reference |
|------------------------------------|-------------------|--------------------------------|
| Bambara groundnut shell | 10 | Ayuba & Nyijime (2021a, 2021b) |
| Chitosan film coated with carbon | 76.9 | Praneesh <i>et al.</i> (2021) |
| Activated Bambara groundnut shells | 14.89 | Ayuba & Nyijime (2021a, 2021b) |
| U-CXSP | 97 | This study |
| AC-CXSP | 114 | This study |
| NM-CXSP | 111 | This study |

$$\frac{t}{q_e} = \frac{1}{k_2 q_e^2} + \frac{t}{q_e} \quad (7)$$

$$qt = k_3 t^{1/2} + c \quad (8)$$

where ' q_t ' indicates the amount of pendimethalin adsorbed by adsorbents at time ' t ' while ' q_e ' indicates the amount of pendimethalin adsorbed by adsorbents at equilibrium, both were measured in mg/g. k_1 , k_2 and k_3 are constants of the respective kinetic models (Shehzad *et al.* 2018).

Pseudo-first-order kinetics was carried out by plotting $\log(q_e - q_t)$ on y-axis and time ' t ' on x-axis. First-order plots for U-CXSP, AC-CXSP and NM-CXSP are shown in Figure 9. Pseudo-second-order kinetics was studied by plotting t/q_e on y-axis and time ' t ' on x-axis. Second-order plots for U-CXSP, AC-CXSP and NM-CXSP are shown in Figure 10. Intraparticle diffusion kinetic model was studied by plotting q_t on y-axis while plotting time ' t ' on x-axis. Plots for intraparticle diffusion are shown in Figure 11. It was seen that the calculated values for adsorption capacity of adsorbent (q_{cal}) were close to the experimental values (q_{exp}) calculated by the pseudo-second-order kinetics. The parameters for these kinetic models were calculated and are shown in Table 3.

3.2.4. Effect of pH and temperature

Effect of pH of solution on the adsorption process was observed by varying the pH of solution between 2 and 10. It is seen that the adsorbents show a good percentage removal in acidic solution and it is maximum at pH = 6. It shows good efficiency in acidic solution which is due to the presence of cellulosic compounds on the adsorbent surface (Ferrero 2007). While in more basic solutions pH > 8, the decrease in percentage adsorption is due to the fact that negatively charged anionic species

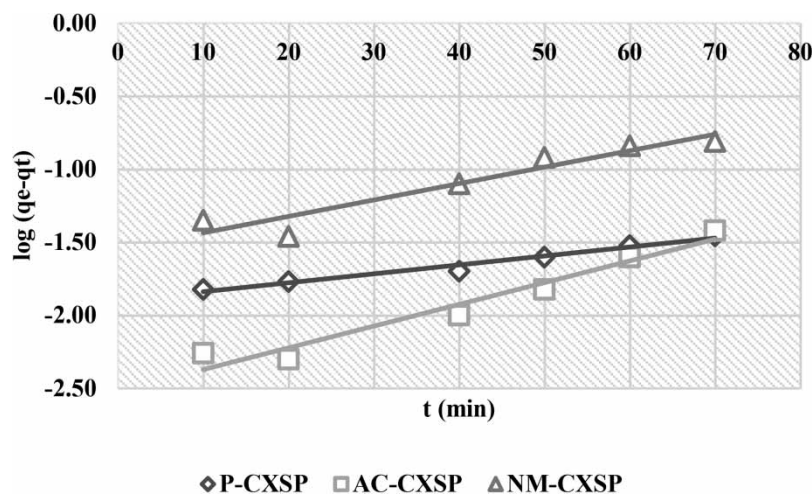


Figure 9 | Pseudo-first-order plots for adsorption of pendimethalin on U-CXSP, AC-CXSP and NM-CXSP. Experimental conditions: temperature = 25 °C, contact time = 30 min, adsorbent dose = 0.1 g, pH = 7.

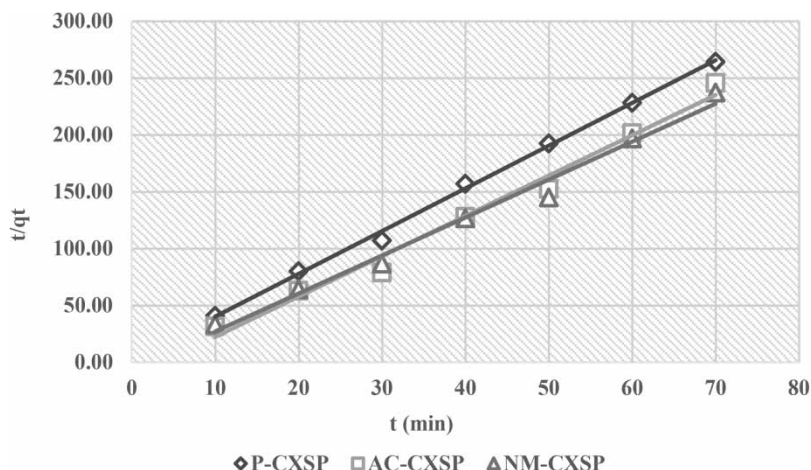


Figure 10 | Pseudo-second-order isotherms for pendimethalin adsorption on (a) U-CXSP, (b) AC-CXSP and (c) NM-CXSP. Experimental conditions: temperature = 25 °C, contact time = 30 min, adsorbent dose = 0.1, pH = 7.

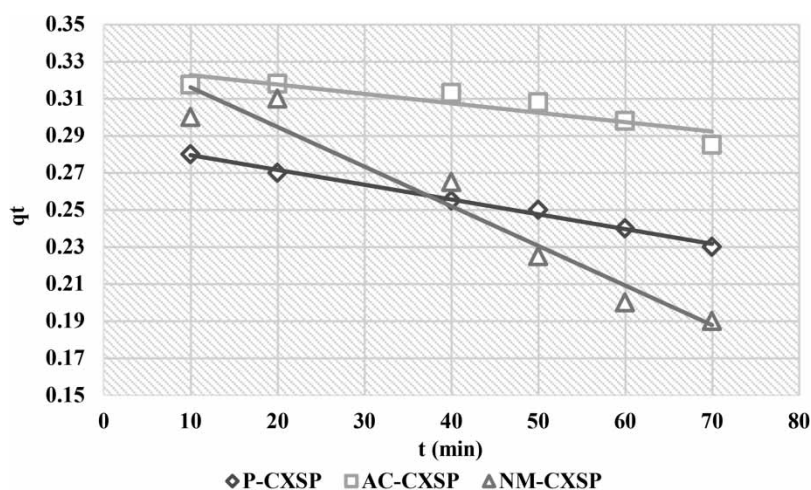


Figure 11 | Intraparticle diffusion plots for pendimethalin adsorption on U-CXSP, AC-CXSP and NM-CXSP. Experimental conditions: temperature = 25 °C, contact time = 30 min, adsorbent dose = 0.1 g, pH = 7.

Table 3 | Kinetic parameters of pendimethalin adsorption on prepared adsorbents

| Pseudo-first-order kinetics | | | | | Pseudo-second-order kinetics | | | Intra particle diffusion | |
|-----------------------------|--------------|-------|--------------|-------|------------------------------|--------------|-------|--------------------------|-------|
| Adsorbent | $q_{e(Exp)}$ | k_1 | $q_{e(Cal)}$ | R^2 | k_2 | $q_{e(Cal)}$ | R^2 | k_3 | R^2 |
| U-CXSP | 0.28 | 0.01 | 0.11 | 0.98 | 0.11 | 0.26 | 0.99 | 0.0003 | 0.98 |
| AC-CXSP | 0.32 | 0.03 | 0.39 | 0.95 | 0.74 | 0.28 | 0.98 | 0.0005 | 0.82 |
| NM-CXSP | 0.35 | 0.03 | 0.18 | 0.98 | 1.22 | 0.30 | 0.98 | 0.0021 | 0.93 |

repel the negative surface of adsorbent under study. The effect of temperature on the uptake of pendimethalin by the prepared adsorbents was studied by keeping the temperature in the range of 25–50 °C. The thickness of the pesticide border on the adsorbent diminishes as the temperature rises. As a consequence, pesticides escaped from the adsorbent surface, resulting in a reduction in pesticide sorption on the adsorbent surface. Results are shown in Figure 12.

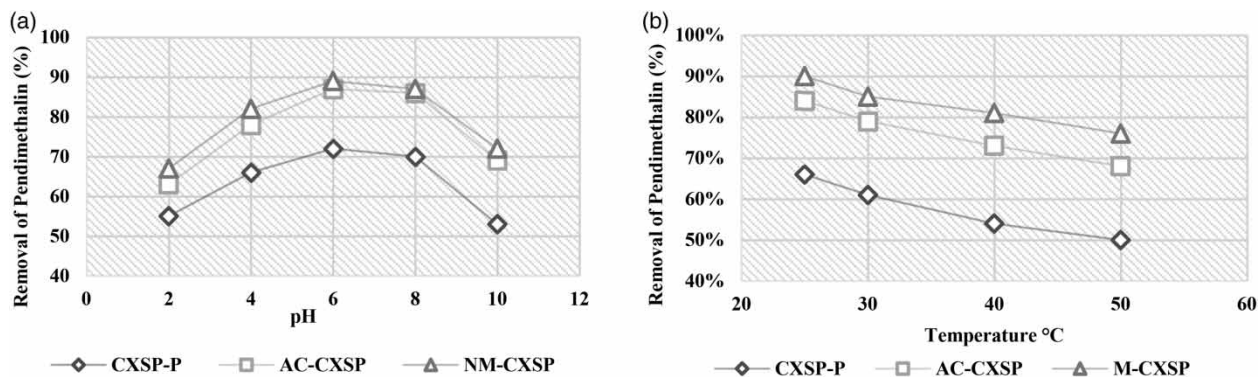


Figure 12 | Effect of (a) pH and (b) temperature on the uptake of pendimethalin (pesticide's concentration = 0.1 ppm, contact time = 30 min, temperature = 25 °C).

Table 4 | Adsorption–desorption cycles

| No. of cycles | Adsorption efficiency (%) | Desorption efficiency (%) |
|---------------|---------------------------|---------------------------|
| 1 | 74.87 | 63.28 |
| 2 | 75.23 | 63.76 |
| 3 | 75.56 | 64.21 |
| 4 | 75.71 | 64.65 |

3.2.5. Adsorption mechanism

Based on kinetics, isotherm and characterization, the adsorption mechanism for this study is provided. Adsorption obeyed second-order kinetics at low (starting) concentrations of adsorbate, as evidenced by the strong relationship between the estimated value of adsorption capacity (q_{cal}) for pseudo-second-order kinetics and the experimental value (q_{exp}). The FTIR study (Abdelhameed *et al.* 2020) verified that the free hydroxyl and carboxylic groups on the surface of the precursor adsorbent (U-CXSP) cause the adsorption of pendimethalin. Research showed that the carbonaceous and magnetized material made from orange peels improved the sorbent's efficacy in absorbing pendimethalin by increasing its surface area. The existence of many microscopic nanoparticles is what causes the rise in NM-CXSP adsorption efficiency. FTIR, VSM and SEM-EDX all indicated the successful formation of NM-CXSP.

3.2.6. Regeneration efficiency of adsorbents

Reusability of the used adsorbents is an important aspect of any cost-effective method. Using a vortex machine, the adsorbents were treated with acetone (2.0 mL) and double distilled water, respectively, to test the adsorption–desorption cycles of the materials for the absorption of pendimethalin. After that, the adsorbents were magnetically collected for further use. In order to assess the adsorbents' efficiency for the adsorption of pendimethalin, Table 4 displays the results from adsorption–desorption cycles. For four cycles, the values for adsorption and desorption were kept within the ranges of 74.87–75.71% and 63.28–64.65%. The outstanding efficiency and reusability of the adsorbents were demonstrated by the experimental findings, which revealed that the adsorption–desorption values were nearly similar. Therefore, it was discovered that the adsorbents employed in this investigation were both efficient and sustainable in cleaning the wastewater containing pendimethalin.

4. CONCLUSION

This study showed that residual pendimethalin present in water bodies as pollutant can successfully be removed by utilizing the biowaste obtained from *Citrus X sinensis* (orange) peels. This is a sustainable approach for the treatment of water resources which utilized low-cost ecofriendly bio-sorbents. The activated carbon and magnetized peels showed a better efficiency for the uptake of pendimethalin as compared to simple fruit peels. The prepared adsorbents were characterized using

SEM, EDX, FTIR, VSM and XRD. All techniques confirmed the formation of nano-magnetized adsorbent. Biosorption studies were carried out by varying different parameters and it was seen that the adsorbents show maximum adsorption with an adsorbent dose 0.4 g, time of contact of 30 min, initial concentration of PDM 80 ppm, pH of 6 and temperature of 25 °C. The results showed that the removal efficiency of U-CXSP increased from 97 to 114 mg/g and to 111 mg/g for AC-CXSP and NM-CXSP adsorbents, respectively. According to the results, the pseudo-second-order kinetic model has the best fit to the experimental data, with a higher correlation coefficient (R^2) than the pseudo-first-order kinetic model. The chemisorption-based pendimethalin adsorption on adsorbents is shown by the best-fit pseudo-second-order equation. Hence, the present work shows *Citrus X sinensis* adsorbents to be promising biomaterials for the removal of pendimethalin from aqueous resources.

DATA AVAILABILITY STATEMENT

All relevant data are included in the paper or its Supplementary Information.

CONFLICT OF INTEREST

The authors declare there is no conflict.

REFERENCES

- Abdelhameed, R. M., Abdel-Gawad, H. & Hegazi, B. 2020 Effective adsorption of prothiofos (O-2, 4-dichlorophenyl O-ethyl S-propyl phosphorodithioate) from water using activated agricultural waste microstructure. *Journal of Environmental Chemical Engineering* **8** (3), 103768.
- Asghar, A., Mabarak, S., Ashraf, B., Rizwan, M., Massey, S., Asghar, B. H., Shahid, B. & Rasheed, T. 2024 A sustainable approach for the removal of chlorpyrifos pesticide from aqueous phase using novel nano magnetized biochar. *Inorganic Chemistry Communications* **159**, 111790.
- Ayuba, A. M. & Nyijime, T. A. 2021 Removal of pendimethalin herbicide from aqueous solution using untreated bambara groundnut hulls as a low-cost adsorbent. *Journal of Materials and Environmental Science* **12**, 15–26.
- Ayuba, A. M. & Nyijime, T. A. 2021 Adsorption and kinetics study for the removal of pendimethalin from aqueous solution using activated carbon prepared from agricultural waste. *Journal of Experimental Research* **9** (2).
- Biswas, B. K., Inoue, J. I., Inoue, K., Ghimire, K. N., Harada, H., Ohto, K. & Kawakita, H. 2008 Adsorptive removal of As (V) and As (III) from water by a Zr (IV)-loaded orange waste gel. *Journal of Hazardous Materials* **154** (1–3), 1066–1074.
- Bulgariu, L., Escudero, L. B., Bello, O. S., Iqbal, M., Nisar, J., Adegoke, K. A., Alakhras, F., Kornaros, M. & Anastopoulos, I. 2019 The utilization of leaf-based adsorbents for dyes removal: A review. *Journal of Molecular Liquids* **276**, 728–747.
- Combo, A. M. M., Aguedo, M., Quiévy, N., Danthine, S., Goffin, D., Jacquet, N., Blecker, C., Devaux, J. & Paquot, M. 2013 Characterization of sugar beet pectic-derived oligosaccharides obtained by enzymatic hydrolysis. *International Journal of Biological Macromolecules* **52**, 148–156.
- Enniya, I., Rghioui, L. & Jourani, A. 2018 Adsorption of hexavalent chromium in aqueous solution on activated carbon prepared from apple peels. *Sustainable Chemistry and Pharmacy* **7**, 9–16.
- Fernandez, M. E., Nunell, G. V., Bonelli, P. R. & Cukierman, A. L. 2014 Activated carbon developed from orange peels: Batch and dynamic competitive adsorption of basic dyes. *Industrial Crops and Products* **62**, 437–445.
- Ferrero, F. 2007 Dye removal by low-cost adsorbents: Hazelnut shells in comparison with wood sawdust. *Journal of Hazardous Materials* **142** (1–2), 144–152.
- Hameed, B. H., Salman, J. M. & Ahmad, A. L. 2009 Adsorption isotherm and kinetic modeling of 2, 4-D pesticide on activated carbon derived from date stones. *Journal of Hazardous Materials* **163** (1), 121–126.
- Jabłońska, B. 2012 Sorption of phenol on rock components occurring in mine drainage water sediments. *International Journal of Mineral Processing* **104**, 71–79.
- Kadam, A. A., Sharma, B., Saratale, G. D., Saratale, R. G., Ghodake, G. S., Mistry, B. M., Shinde, S. K., Jee, S. C. & Sung, J. S. 2020 Super-magnetization of pectin from orange-peel biomass for sulfamethoxazole adsorption. *Cellulose* **27** (6), 3301–3318.
- Kumar, M. & Philip, L. 2006 Adsorption and desorption characteristics of hydrophobic pesticide endosulfan in four Indian soils. *Chemosphere* **62** (7), 1064–1077.
- Kushwaha, S., Soni, H., Ageetha, V. & Padmaja, P. 2013 An insight into the production, characterization, and mechanisms of action of low-cost adsorbents for removal of organics from aqueous solution. *Critical Reviews in Environmental Science and Technology* **43** (5), 443–549.
- Memon, G. Z., Bhangar, M. I., Akhtar, M., Talpur, F. N. & Memon, J. R. 2008 Adsorption of methyl parathion pesticide from water using watermelon peels as a low-cost adsorbent. *Chemical Engineering Journal* **138** (1–3), 616–621.
- Mohammad, S. G., Ahmed, S. M. & Badawi, A. F. M. 2015 A comparative adsorption study with different agricultural waste adsorbents for removal of oxamyl pesticide. *Desalination and Water Treatment* **55** (8), 2109–2120.

- Moradi, O., Norouzi, M., Fakhri, A. & Naddafi, K. 2014 Interaction of removal ethidium bromide with carbon nanotube: Equilibrium and isotherm studies. *Journal of Environmental Health Science and Engineering* **12** (1), 1–9.
- Nandiyanto, A. B. D., Oktiani, R. & Ragadhita, R. 2019 How to read and interpret FTIR spectroscopy of organic material. *Indonesian Journal of Science and Technology* **4** (1), 97–118.
- Praneesh, M., Babu, V. & Anu, G. A. 2021 A green technology for the removal of pendimethalin from aqueous system using adsorption technique. *Pollution Research* **40** (1), 182–188.
- Ren, L., Zhang, J., Li, Y. & Zhang, C. 2011 Preparation and evaluation of cattail fiber-based activated carbon for 2, 4-dichlorophenol and 2, 4, 6-trichlorophenol removal. *Chemical Engineering Journal* **168** (2), 553–561.
- Salman, J. M., Njoku, V. O. & Hameed, B. H. 2011 Adsorption of pesticides from aqueous solution onto banana stalk activated carbon. *Chemical Engineering Journal* **174** (1), 41–48.
- Shehzad, K., Xie, C., He, J., Cai, X., Xu, W. & Liu, J. 2018 Facile synthesis of novel calcined magnetic orange peel composites for efficient removal of arsenite through simultaneous oxidation and adsorption. *Journal of Colloid and Interface Science* **511**, 155–164.
- Sheng, T., Baig, S. A., Hu, Y., Xue, X. & Xu, X. 2014 Development, characterization and evaluation of iron-coated honeycomb briquette cinders for the removal of As (V) from aqueous solutions. *Arabian Journal of Chemistry* **7** (1), 27–36.
- Siddique, A., Nayak, A. K. & Singh, J. 2020 Synthesis of FeCl₃-activated carbon derived from waste Citrus limetta peels for removal of fluoride: An eco-friendly approach for the treatment of groundwater and bio-waste collectively. *Groundwater for Sustainable Development* **10**, 100339.

First received 19 June 2023; accepted in revised form 16 January 2024. Available online 20 February 2024